

Molecular Epidemiology of Mayaro Virus among Febrile Patients, Roraima State, Brazil, 2018–2021

Julia Forato, Cássio A. Meira, Ingra M. Claro, Mariene R. Amorim, Gabriela F. de Souza, Stefanie P. Muraro, Daniel A. Toledo-Teixeira, Miguel F. Dias, Cátia A. R. Meneses, Rodrigo N. Angerami, Pritesh Lalwani, Scott C. Weaver, Ester C. Sabino, Nuno R. Faria, William M. de Souza,¹ Fabiana Granja,¹ José Luiz Proenca-Modena¹

We detected Mayaro virus (MAYV) in 3.4% (28/822) of febrile patients tested during 2018–2021 from Roraima State, Brazil. We also isolated MAYV strains and confirmed that these cases were caused by genotype D. Improved surveillance is needed to better determine the burden of MAYV in the Amazon Region.

Mayaro virus (MAYV) is an endemic and neglected mosquito-borne alphavirus that causes acute and chronic debilitating arthritogenic disease in Latin America and the Caribbean (1). MAYV infection can cause fever, rash, and arthralgia that can persist for over a year in some patients (2). MAYV is transmitted in its enzootic cycle mainly by sylvatic *Haemagogus janthinomys* mosquitoes among nonhuman primates and other mammals, which can lead to spillover to humans (2). However, some experimental studies suggest that MAYV could establish a human-amplified cycle in urban environments when transmitted by *Aedes aegypti* and *Ae. albopictus* mosquitoes, which

could lead to a larger public health threat (3,4). No specific antiviral drugs or vaccines are available to treat or prevent MAYV infection.

MAYV infections have been reported in Central and South America since the 1950s (1,2). However, reports of active circulation of MAYV in human populations remain scarce, even in MAYV-endemic areas. We conducted a molecular epidemiology study to investigate the active circulation of MAYV in patients with acute febrile illness during 2018–2021 from the Amazon Region in Roraima State, Brazil.

The Study

During December 2018–December 2021, we collected serum samples from 822 patients with acute febrile illness (up to 10 days from onset of symptoms) seeking care at primary health care units across 11 of the 15 municipalities of Roraima State, North Region, Brazil. We collected patient information, such as age, sex, occupation, sample collection data, date of symptom onset, and symptoms, from medical records. We conducted all procedures in accordance with ethics committee approval from the Federal University of Roraima (approval no. 2.881.239) and the University of Campinas (approval no. 5.625.875).

Next, we extracted RNA from all serum samples and performed real-time reverse transcription PCR (rRT-PCR) to detect RNA of MAYV, chikungunya virus (CHIKV), Zika virus, dengue virus (DENV), and Oropouche virus. We also carried out viral isolation in African green monkey kidney cells (Vero CCL-81) with some positive samples. Then, we performed sequencing by using the nanopore approach (5) and conducted maximum-likelihood phylogenetic

Author affiliations: Universidade Estadual de Campinas, Campinas, São Paulo, Brazil (J. Forato, M.R. Amorim, D.A. Toledo-Teixeira, R.N. Angerami, F. Granja, J.L. Proenca-Modena); Laboratório Central de Saúde Pública de Roraima, Boa Vista, Brazil (C.A. Meira, C.A.R. Meneses); University of São Paulo, São Paulo (I.M. Claro, E.C. Sabino, N.R. Faria); Imperial College London, London, UK (I.M. Claro, N.R. Faria); University of Kentucky, Lexington, Kentucky, USA (W.M. de Souza); Global Virus Network, Baltimore, Maryland, USA (W.M. de Souza, S.C. Weaver); Federal University of Roraima, Boa Vista (M.F. Dias, F. Granja); Fiocruz Amazônia, Manaus, Brazil (P. Lalwani); University of Texas Medical Branch, Galveston, Texas, USA (S.C. Weaver); University of Oxford, Oxford, UK (N.R. Faria)

DOI: <https://doi.org/10.3201/eid3005.231406>

¹These senior authors contributed equally to this article.

inferences (Appendix, <https://wwwnc.cdc.gov/EID/article/30/5/23-1406-App1.pdf>).

Of 822 patients tested by rRT-PCR, 190 (23.1%) were positive for ≥ 1 arbovirus (Appendix Figure 1). We detected MAYV RNA in 28 (3%) patients, including 15 (54%) patients from Boa Vista, the most populous municipality in Roraima State (Appendix Figure 2). Most (19 [68%]) MAYV cases occurred during January–July 2021. Among patients with rRT-PCR-confirmed MAYV, median age was 31 years (interquartile range 26–43 years), and the male-to-female ratio was 1:5. The most common signs and symptoms reported were fever and myalgia, both of which were reported in 23 (82%) MAYV cases. Arthralgia was reported in 6 (21%) and rash in 3 (11%) cases. The median time between symptom onset and sample collection interval was 3 days (interquartile range 1–4 days). Three (11%) of the MAYV cases were in fishermen who had direct contact with wildlife.

Next, we isolated 2 MAYV strains in Vero CCL-81 cells, and we observed cytopathic effects (CPE) ≈ 30 hours after inoculation. Then, we performed 3 blind passages and confirmed the viral isolation of 2 strains by using rRT-PCR to detect viral RNA in the supernatant of culture cell passages exhibiting CPE. We observed decreased cycle threshold values representing increased viral loads between passages (Appendix Figure 3). In addition, we confirmed MAYV isolates by using immunofluorescent staining (Appendix Figure 4). Subsequently, we used nanopore sequencing to generate the nearly complete coding sequencing of 3 MAYV strains (2 isolates and 1 directly from a clinical sample). We obtained $>90\%$ of MAYV genomes with a mean depth of coverage of ≥ 20 -folds per nucleotide. We submitted sequences to GenBank (accession nos. PP339762–PP339764).

The maximum-likelihood phylogenetic analysis showed that the MAYV strains circulating in Roraima

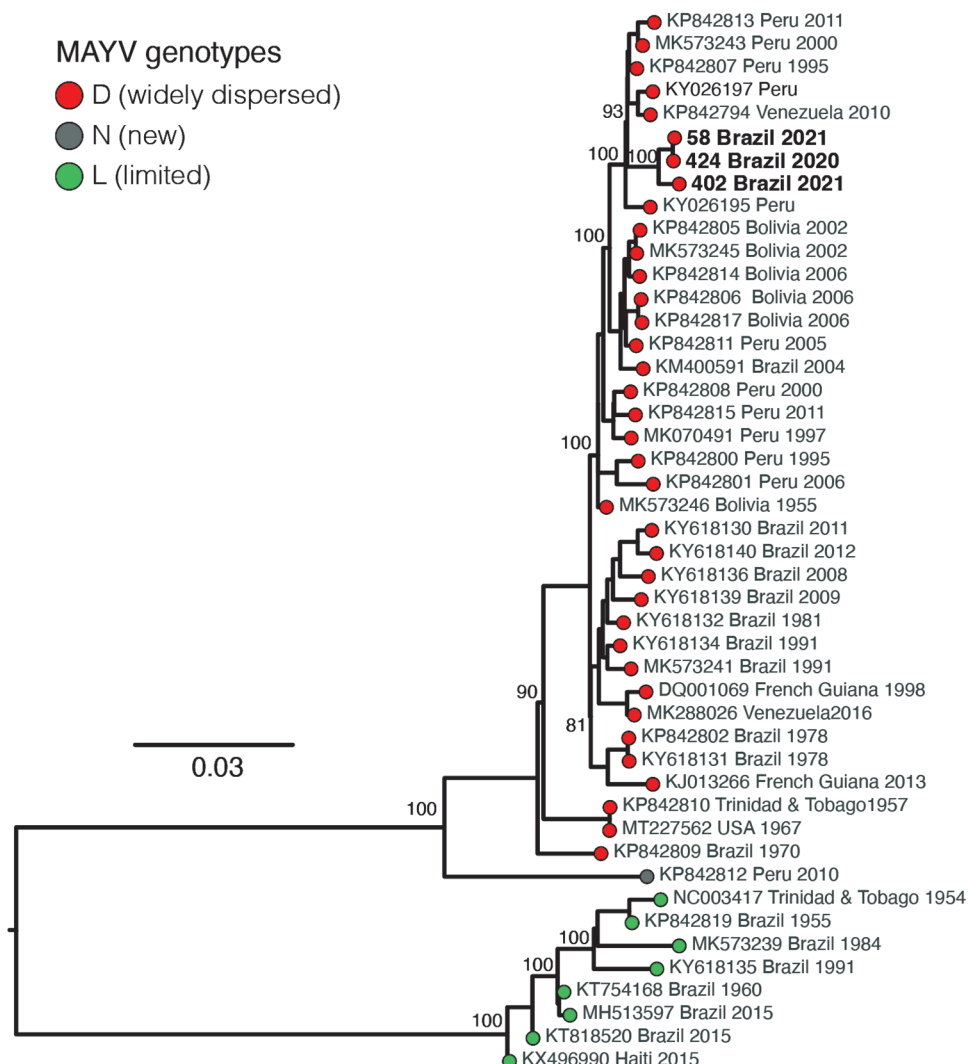


Figure. Maximum-likelihood phylogenetic tree of Mayaro virus, Roraima State, Brazil, 2018–2021. Phylogeny is midpoint rooted for clarity of presentation. Bold text indicates 3 new Mayaro virus genomes. Bootstrap values based on 1,000 replicates are shown on principal nodes. Scale bar indicates the evolutionary distance of substitutions per nucleotide site.

State in 2021 belong to genotype D (widely dispersed) (Figure). We identified no evidence of recombination in MAYV strains from Roraima State. The novel MAYV strains shared 98.6%–98.9% nucleotide sequence identity with other genotype D strains. The new strains formed a distinct and highly supported monophyletic clade (bootstrap support 100%) and clustered with strains sampled in Peru and Venezuela during 1995–2010.

Finally, we also detected CHIKV RNA in 16 (2%) and DENV in 146 (17.8%) patients tested (Appendix Figures 1, 5). This number includes 63 patients with DENV serotype 1 and 89 patients with DENV serotype 2. Of those, we identified 6 (1%) cases with co-detection of DENV-1 and DENV-2. We detected most (13 [81%]) chikungunya cases in patients with febrile illness during January–July 2021, overlapping with the peak of detection for MAYV. Conversely, dengue cases were predominantly confirmed (110 [75.3%]) in patients with fever during July 2019–January 2020. All samples tested were negative for RNA of Zika virus, Oropouche viruses, and DENV serotypes 3 and 4.

Conclusions

This study reports the active MAYV circulation in humans during the concurrent chikungunya and dengue epidemic in Roraima State, Brazil. We found that the MAYV infection cases were caused by genotype D, suggesting that this widespread genotype continued to circulate in the Amazon Region for ≥ 60 years. In addition, this same genotype has been detected in outbreaks in Venezuela (6,7), which, like Guyana, shares borders with Brazil through Roraima State.

Arthralgia has been described as a major clinical characteristic of human MAYV infection (8). However, only 21% of MAYV-positive patients reported arthralgia in this study. Our data suggest that laboratory diagnosis of MAYV should be considered for patients with febrile illness in MAYV-endemic areas, even in the absence of clinical characteristics typically associated with MAYV infection. We also found that young adults and men account for most of the MAYV infection cases, probably because of occupational exposure (9). Persons who work in forest environments (e.g., in mining, logging, and fishing) could be a bridge to facilitate the eventual introduction and establishment of MAYV transmission in urban settings (7). Moreover, the implementation of augmented molecular and genomic surveillance in human and urban vector populations (i.e., *Ae. aegypti* and *Ae. albopictus* mosquitoes) will be critical to monitor the

potential establishment of MAYV in a human-amplified transmission cycle.

One limitation of our study is that we focused on active MAYV infections by using a molecular approach; however, further serologic studies are needed to determine the fraction of the population previously infected. Serologic studies can shed light on the potential effect of cross-protection between CHIKV and MAYV in the Amazon Region (10). Moreover, the higher percentage (76.9%) of samples negative for the arboviruses tested shows that the metagenomic approach could be useful in further studies to determine the landscape of etiologic agents linked with febrile illness in the triple border region (i.e., Brazil, Guyana, and Venezuela). Further, we were unable to determine whether MAYV infections occurred in urban or forest settings, and we have no follow-up information on MAYV cases.

In conclusion, our study identified the active co-circulation of MAYV, DENV, and CHIKV in patients with febrile illness in Roraima State, Brazil. These findings underscore the critical need for continuous laboratory diagnosis for MAYV to determine the prevalence of MAYV in the Amazon Region and the potential changes associated with urbanization.

Acknowledgments

We thank Clarice Arns for her technical support and Rafael Elias Marques for providing the Mayaro and dengue virus isolates.

This study was supported by grants from São Paulo Research Foundation (grant nos. 2016/00194-8, 2020/04558-0, and 2022/10442-0). J.F. was supported by Coordination for the Improvement of Higher Education Personnel scholarships (grant no. 309971/2023-3). W.M.d.S. was supported by a Global Virus Network fellowship, Burroughs Wellcome Fund (grant no. 1022448), and Wellcome Trust-Digital Technology Development award (climate sensitive infectious disease modelling, under grant no. 226075/Z/22/Z). I.M.C. was supported by São Paulo Research Foundation (grant no. 2018/17176-8) and the Bill and Melinda Gates Foundation (grant no. INV-034540). S.C.W. was supported by the National Institutes of Health (grant nos. AI12094, U01AI151801, and AI121452). J.L.P.-M. is supported by Conselho Nacional de Desenvolvimento Científico e Tecnológico (grant no. 305628/2020-8). This project was supported by the Medical Research Council and São Paulo Research Foundation Centre for Arbovirus Discovery, Diagnosis, Genomics and Epidemiology partnership award (grant nos. MR/S0195/1 and FAPESP 2018/14389-0).

About the Author

Ms. Forato is a master's candidate at the Department of Genetics, Evolution, Microbiology, and Immunology at the University of Campinas, São Paulo, Brazil. Her research interests include epidemiologic surveillance of emerging viruses with a focus on arboviruses.

References

1. Caicedo EY, Charniga K, Rueda A, Dorigatti I, Mendez Y, Hamlet A, et al. The epidemiology of Mayaro virus in the Americas: a systematic review and key parameter estimates for outbreak modelling. *PLoS Negl Trop Dis*. 2021;15:e0009418. <https://doi.org/10.1371/journal.pntd.0009418>
2. Hoch AL, Peterson NE, LeDuc JW, Pinheiro FP. An outbreak of Mayaro virus disease in Belterra, Brazil. III. Entomological and ecological studies. *Am J Trop Med Hyg*. 1981;30:689–98. <https://doi.org/10.4269/ajtmh.1981.30.689>
3. Fernández D, Yun R, Zhou J, Parise PL, Mosso-González C, Villasante-Tezanos A, et al. Differential susceptibility of *Aedes aegypti* and *Aedes albopictus* mosquitoes to infection by Mayaro virus strains. *Am J Trop Med Hyg*. 2023;109:115–22. <https://doi.org/10.4269/ajtmh.22-0777>
4. Weaver SC. Urbanization and geographic expansion of zoonotic arboviral diseases: mechanisms and potential strategies for prevention. *Trends Microbiol*. 2013;21:360–3. <https://doi.org/10.1016/j.tim.2013.03.003>
5. Claro IM, Ramundo MS, Coletti TM, da Silva CAM, Valença IN, Candido DS, et al. Rapid viral metagenomics using SMART-9N amplification and nanopore sequencing. *Wellcome Open Res*. 2023;6:241. <https://doi.org/10.12688/wellcomeopenres.17170.2>
6. Auguste AJ, Liria J, Forrester NL, Giambalvo D, Moncada M, Long KC, et al. Evolutionary and ecological characterization of Mayaro virus strains isolated during an outbreak, Venezuela, 2010. *Emerg Infect Dis*. 2015;21:1742–50. <https://doi.org/10.3201/eid2110.141660>
7. Guégan JF, Ayoub A, Cappelle J, De Thoisy B. Forests and emerging infectious diseases: unleashing the beast within [cited 2023 Aug 17]. <https://iopscience.iop.org/article/10.1088/1748-9326/ab8dd7>
8. Halsey ES, Siles C, Guevara C, Vilcarromero S, Jhonston EJ, Ramal C, et al. Mayaro virus infection, Amazon Basin region, Peru, 2010–2013. *Emerg Infect Dis*. 2013;19:1839–42. <https://doi.org/10.3201/eid1911.130777>
9. Forshey BM, Guevara C, Laguna-Torres VA, Cespedes M, Vargas J, Gianella A, et al.; NMRCD Febrile Surveillance Working Group. Arboviral etiologies of acute febrile illnesses in western South America, 2000–2007. *PLoS Negl Trop Dis*. 2010;4:e787. <https://doi.org/10.1371/journal.pntd.0000787>
10. Fumagalli MJ, de Souza WM, de Castro-Jorge LA, de Carvalho RVH, Castro ÍA, de Almeida LGN, et al. Chikungunya virus exposure partially cross-protects against Mayaro virus infection in mice. *J Virol*. 2021;95:e0112221. <https://doi.org/10.1128/JVI.01122-21>

Address for correspondence: Julia Forato, Universidade Estadual de Campinas, Rua Monteiro Lobato, No. 255, 13.083-862, Campinas, São Paulo, Brazil; email: foratojulia@gmail.com

EID Podcast

Angiostrongylus cantonensis Infection in Brown Rats (*Rattus norvegicus*), Atlanta, Georgia, USA, 2019–2022



Rat lungworm (*Angiostrongylus cantonensis*), causes eosinophilic meningoencephalitis in people and other accidental mammal hosts. Tissue samples were collected from wild brown rats found dead during 2019–2022 on the grounds of a zoological facility in Atlanta, Georgia, and were confirmed to be infected with *A. cantonensis*. This discovery suggests that this zoonotic parasite was introduced to and has become established in a new area of the southeastern United States.

In this EID podcast, Dr. Guilherme Verocai, a clinical assistant professor at Texas A&M University, discusses rat lungworm infection in brown rats in Atlanta, Georgia.

Visit our website to listen:
<https://bit.ly/3RAdwLC>

**EMERGING
 INFECTIOUS DISEASES®**

Molecular Epidemiology of Mayaro Virus among Febrile Patients, Roraima State, Brazil, 2018–2021

Appendix

Materials and Methods

Blood Samples Collection

Blood samples from patients with acute febrile illness (up to 10 days from onset symptoms) were collected by venipuncture at primary health care units in 11 of the 15 municipalities of Roraima State, Brazil. Next, the samples were sent to the Central Public Health Laboratory to investigate the etiological agent. Lastly, residual serum samples from 822 patients with a volume between 0.2 and 2 mL were provided for this study. All samples were stored at -80°C .

Real-time Quantitative Reverse Transcription-PCR (RT-qPCR) for Mayaro, Chikungunya, Dengue, Zika, and Oropouche Viruses

Viral RNA was extracted from the serum samples using the QIAamp Viral RNA Mini Kit (QIAGEN, USA) following the manufacturer's instructions. Then, RNA extracted was tested by real-time RT-qPCR targeting Mayaro (MAYV) (1), chikungunya (CHIKV) (2), dengue serotypes 1 to 4 (DENV 1-4) (3,4), Zika (ZIKV) (5), and Oropouche viruses (OROV) (6) using the TaqMan RNA to-CT 1-Step Kit (Applied Biosystems, USA) and qPCR BIO Probe 1-Step Go Lo - ROX Kit (PCR Biosystems, UK). Reactions were performed on QuantStudio 3 (Applied Biosystems, USA). The primers and probes used for the viral detection are described (Appendix Table 1).

Virus Isolation

Nine serum samples that tested positive for RNA MAYV via RT-qPCR were inoculated into Vero cells (CCL-81) for viral isolation (Appendix Table 2). We observed viral growth in 2 samples inoculated ($\approx 22\%$, 2/9). Briefly, Vero cells were plated in six-well plates at a concentration of 1×10^6 cells per ml (1×10^6 cells per well) in Minimum Essential Eagle's Medium (DMEM), supplemented with 10% fetal bovine serum (FBS), and 1% of penicillin of 10,000 units and 10,000 $\mu\text{g/ml}$ streptomycin solution. Subsequently, the serum samples ($n=9$) were diluted 1:10 in DMEM, treated with 2% penicillin and streptomycin and added to the monolayer. After a one-hour incubation at 37°C for adsorption, the inoculum was removed, and the monolayer was maintained in DMEM supplemented with 5% FBS. The cells were kept at 37°C with 5% CO_2 and monitored for 30 hours until the cytopathic effect (CPE) became visible on an optical microscope. Next, the supernatant was collected and subjected to an RT-qPCR assay (*I*) to confirm viral isolation (two samples), indicated by a decrease in the Ct-value.

Mayaro Virus Genome Sequencing and Analysis

MAYV genome sequencing was performed with samples and isolates with Ct values <30 using the Rapid SMART-9N protocol with the MinION platform (Oxford Nanopore Technologies, UK), as previously described (7). The generated raw FAST5 files were then basecalled, demultiplexed, and trimmed using Guppy version 9.4.1 (Oxford Nanopore Technologies, UK). The barcoded files were aligned to the MAYV reference genome (GenBank accession no. NC_003417) using minimap2 v.2.17.r941 (8) and converted into BAM files using SAMtools (9). Medaka_variants were employed for variant calling, followed by medaka_consensus (Oxford Nanopore Technologies, UK) for consensus sequence building. Genome regions with coverage below $20\times$ were represented by the letter "N". NanoStat version 1.6.0, Samtools stats, and samtools depth (10) were applied to compute the genome statistics.

Phylogenetic Analysis

The three novel MAYV genomes with $>90\%$ coverage were generated and aligned with the non-redundant MAYV strains with complete coding sequences available in the GenBank database as of September 15, 2023. Then, we performed a multiple sequence alignment (MSA) built using MAFFT version 7.450 (11), and manual adjustment was conducted using Geneious Prime 2023.0.4. The dataset was screened for recombination events using all available methods in RDP version 4 (12), but no evidence of recombination was found. A maximum-likelihood

(ML) phylogeny tree was performed using IQ-TREE version 2 under a GTR + I + γ model determined by ModelFinder (13,14). The ultrafast-bootstrap approach with 1,000 replicates was used to determine the statistical support for nodes for the ML phylogeny. The phylogenetic tree was visualized using Figtree 1.4.2 (<http://tree.bio.ed.ac.uk/software/figtree/>).

Immunofluorescence Assay

The immunofluorescence assays were conducted using the MAYV isolate #1 from patient RR-736. Briefly, Vero cells (CCL-81) were cultured in chamber slides at a concentration of 5×10^5 cells per mL (1×10^5 cells per well) in DMEM, supplemented with 10% FBS and 1% of a 1:1 mixture of penicillin (10,000 units/ml) and streptomycin (10,000 $\mu\text{g}/\text{mL}$), and incubated in a 37°C incubator with 5% CO₂ for 24 hours. Subsequently, the cells were infected with the MAYV isolate #1 for 1 hour using a multiplicity of infection (MOI) of 1. For the assay, cells were first blocked with 5% bovine serum albumin (BSA) solution and incubated with BD Cytotfix/Cytoperm Fixation and Permeabilization Solution (Becton Dickson, EUA). Afterward, the primary antibodies anti-Mayaro virus E2 antibody, clone MAY-134 (Merk, USA), and anti-Vimentin antibody (ABCAM, USA), both at a dilution of 1:100, were added and incubated for 2 hours at room temperature. Next, cells were incubated with secondary antibodies goat anti-rabbit IgG AF750 (ABCAM, USA) and goat anti-mouse IgG AF594 (Thermo Fisher Scientific, USA), both at a dilution of 1:500, for 1 hour at room temperature protected from light. Hoechst dye was added for 20 minutes at room temperature for nuclear staining, also protected from light. Finally, coverslips were mounted using Fluoromount-G Mounting Medium (Invitrogen, USA), and images were obtained using the Leica TCS SP5 II confocal microscope at a magnification of 20 \times (Leica, Germany) in the Central Laboratory for High-Performance Life Sciences Technologies at the Universidade Estadual de Campinas, Brazil.

References

1. Waggoner JJ, Rojas A, Mohamed-Hadley A, de Guillén YA, Pinsky BA. Real-time RT-PCR for Mayaro virus detection in plasma and urine. *J Clin Virol.* 2018;98:1–4. [PubMed](https://doi.org/10.1016/j.jcv.2017.11.006)
<https://doi.org/10.1016/j.jcv.2017.11.006>
2. Lanciotti RS, Kosoy OL, Laven JJ, Panella AJ, Velez JO, Lambert AJ, et al. Chikungunya virus in US travelers returning from India, 2006. *Emerg Infect Dis.* 2007;13:764–7. [PubMed](https://doi.org/10.3201/eid1305.070015)
<https://doi.org/10.3201/eid1305.070015>

3. Callahan JD, Wu SJL, Dion-Schultz A, Mangold BE, Peruski LF, Watts DM, et al. Development and evaluation of serotype- and group-specific fluorogenic reverse transcriptase PCR (TaqMan) assays for dengue virus. *J Clin Microbiol.* 2001;39:4119–24. [PubMed](#)
<https://doi.org/10.1128/JCM.39.11.4119-4124.2001>
4. Johnson BW, Russell BJ, Lanciotti RS. Serotype-specific detection of dengue viruses in a fourplex real-time reverse transcriptase PCR assay. *J Clin Microbiol.* 2005;43:4977–83. [PubMed](#)
<https://doi.org/10.1128/JCM.43.10.4977-4983.2005>
5. Balm MND, Lee CK, Lee HK, Chiu L, Koay ESC, Tang JW. A diagnostic polymerase chain reaction assay for Zika virus. *J Med Virol.* 2012;84:1501–5. [PubMed](#) <https://doi.org/10.1002/jmv.23241>
6. de Souza Luna LK, Rodrigues AH, Santos RIM, Sesti-Costa R, Criado MF, Martins RB, et al. Oropouche virus is detected in peripheral blood leukocytes from patients. *J Med Virol.* 2017;89:1108–11. [PubMed](#) <https://doi.org/10.1002/jmv.24722>
7. Claro IM, Ramundo MS, Coletti TM, da Silva CAM, Valenca IN, Candido DS, et al. Rapid viral metagenomics using SMART-9N amplification and nanopore sequencing. *Wellcome Open Res.* 2023;6:241. [PubMed](#) <https://doi.org/10.12688/wellcomeopenres.17170.2>
8. Li H. Minimap2: pairwise alignment for nucleotide sequences. *Bioinformatics.* 2018;34:3094–100. [PubMed](#) <https://doi.org/10.1093/bioinformatics/bty191>
9. Li H, Handsaker B, Wysoker A, Fennell T, Ruan J, Homer N, et al.; 1000 Genome Project Data Processing Subgroup. The sequence alignment/map format and SAMtools. *Bioinformatics.* 2009;25:2078–9. [PubMed](#) <https://doi.org/10.1093/bioinformatics/btp352>
10. De Coster W, D’Hert S, Schultz DT, Cruts M, Van Broeckhoven C. NanoPack: visualizing and processing long-read sequencing data. *Bioinformatics.* 2018;34:2666–9. [PubMed](#)
<https://doi.org/10.1093/bioinformatics/bty149>
11. Katoh K, Standley DM. MAFFT multiple sequence alignment software version 7: improvements in performance and usability. *Mol Biol Evol.* 2013;30:772–80. [PubMed](#)
<https://doi.org/10.1093/molbev/mst010>
12. Martin DP, Varsani A, Roumagnac P, Botha G, Maslamoney S, Schwab T, et al. RDP5: a computer program for analyzing recombination in, and removing signals of recombination from, nucleotide sequence datasets. *Virus Evol.* 2020;7:a087. [PubMed](#) <https://doi.org/10.1093/ve/veaa087>

13. Nguyen LT, Schmidt HA, von Haeseler A, Minh BQ. IQ-TREE: a fast and effective stochastic algorithm for estimating maximum-likelihood phylogenies. *Mol Biol Evol.* 2015;32:268–74.

[PubMed https://doi.org/10.1093/molbev/msu300](https://doi.org/10.1093/molbev/msu300)

14. Kalyaanamoorthy S, Minh BQ, Wong TKF, von Haeseler A, Jermin LS. ModelFinder: fast model selection for accurate phylogenetic estimates. *Nat Methods.* 2017;14:587–9. [PubMed https://doi.org/10.1038/nmeth.4285](https://doi.org/10.1038/nmeth.4285)

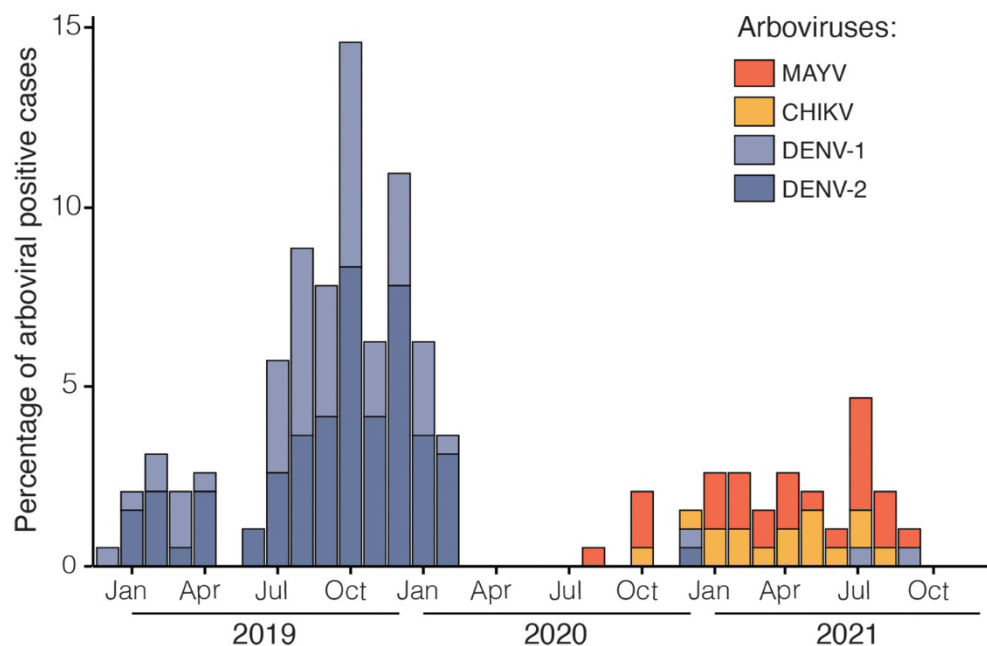
Appendix Table 1. Primers and probes used for the detection of arboviruses in this study

Virus	Sequences (5'→3')	Primers and probes	Target	Genome position	Reference
ZIKV	AARTACACATACCARAACAAAGTGGT	Forward	NS5	9365–9390	Balm et al., 2012 (5)
Xx	TCCRCTCCCYCTYTGGTCTTG	Reverse	NS5	9466–9446	
Xx	CTYAGACCAGCTGAAR	Probe		9398–9413	
DENV1	GACACCACACCCTTTGGACAA	Forward	NS5	8586–8606	Callahan et al., 2001 (3)
Xx	CACYTGGGCTGTCACCTCCAT	Reverse	NS5	8692–8673	
Xx	AGAGGGTGTTTAAAGAGAAAGTTGACACGCG	Probe		8608–8638	
DENV2	CAGTTATGGCACTGTCAGAT	Forward	M	1605	Johnson et al., 2005 (4)
Xx	CCATCTGCAGCAACACCATCTC	Reverse	M	1583	
Xx	CTCCGAGAACAGCCTCGACTTCAA	Probe		1008	
DENV3	GGGAAAACCGTCTATCAATA	Forward	C	118–221	Callahan et al., 2001 (3)
Xx	CGCCATAACCAATTTTCATTGG	Reverse	C	241–221	
Xx	CACAGTTGGCGAAGAGATCTCAAGAGGA	Probe		174–202	
DENV4	TGAAGAGATTCTCAACCGGAC	Forward	C	187–207	Callahan et al., 2001 (3)
Xx	AATCCCTGCTGTTGGTGGC	Reverse	C	293–275	
Xx	TCATCACGTTTTTGCAGTCTTTCCA	Probe		247–273	
CHIKV	AAAGGGCAAACCTCAGCTTCAC	Forward	NSP1	874–894	Lanciotti et al., 2007 (2)
Xx	GCCTGGGCTCATCGTTATTC	Reverse	NSP1	961–942	
Xx	CGCTGTGATACAGTGGTTTCGTGTG	Probe		899–923	
MAYV	AAGCTCTTCTCTGCATTGC	Forward	NSP1	51–70	Waggoner et al., 2018 (1)
Xx	TGCTGGAAACGCTCTCTGTA	Reverse1	NSP1	141–160	
Xx	TGCTGGAAATGCTCTTTGTA	Reverse2		141–160	
Xx	GCCGAGAGCCCGTTTTTAAATCA	Probe		116–140	
OROV	TACCCAGATGCGATCACCAA	Forward	N	356–375	de Souza Luna et al., 2017 (6)
Xx	TTGCGTCACCATCATTCCAA	Reverse	N	437–456	
Xx	TGCCTTTGGCTGAGGTAAGGGCT	Probe		409–433	

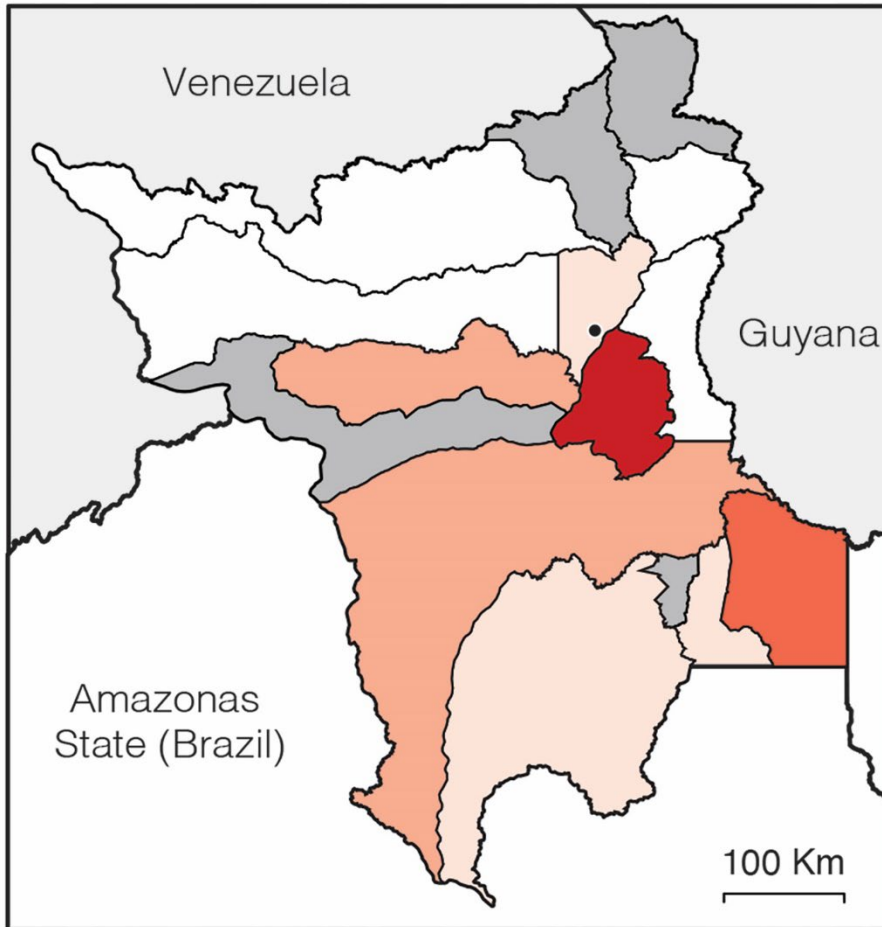
C, capsid protein; CHIKV, chikungunya virus; DENV, dengue virus; M, matrix protein; MAYV, Mayaro virus; N, nucleoprotein; NSP1, non-structural protein 1; NS5, non-structural protein 5; OROV, Oropouche virus; ZIKV, Zika virus.

Appendix Table 2. Information of MAYV confirmed cases by RT-PCR

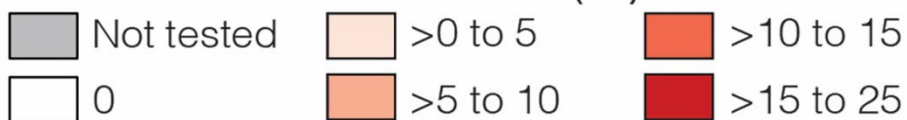
Sample ID	Cycle threshold value	Viral isolation
469	40.00	Not performed
470	39.03	Not performed
472	39.29	Not performed
20	38.82	Failed
21	39.98	Not performed
22	39.71	Not performed
49	39.17	Not performed
58	27.03	Successful (Viral growth)
90	39.70	Not performed
92	40.53	Not performed
120	39.87	Not performed
127	40.43	Not performed
166	39.69	Not performed
240	38.90	Failed
285	39.36	Not performed
310	38.03	Failed
329	39.42	Not performed
336	39.34	Not performed
340	39.26	Not performed
352	39.48	Not performed
360	39.43	Not performed
402	36.82	Failed
430	39.23	Not performed
458	39.40	Not performed
396	37.96	Failed
424	30.35	Successful (Viral growth)
66	31.03	Failed
315	33.76	Failed



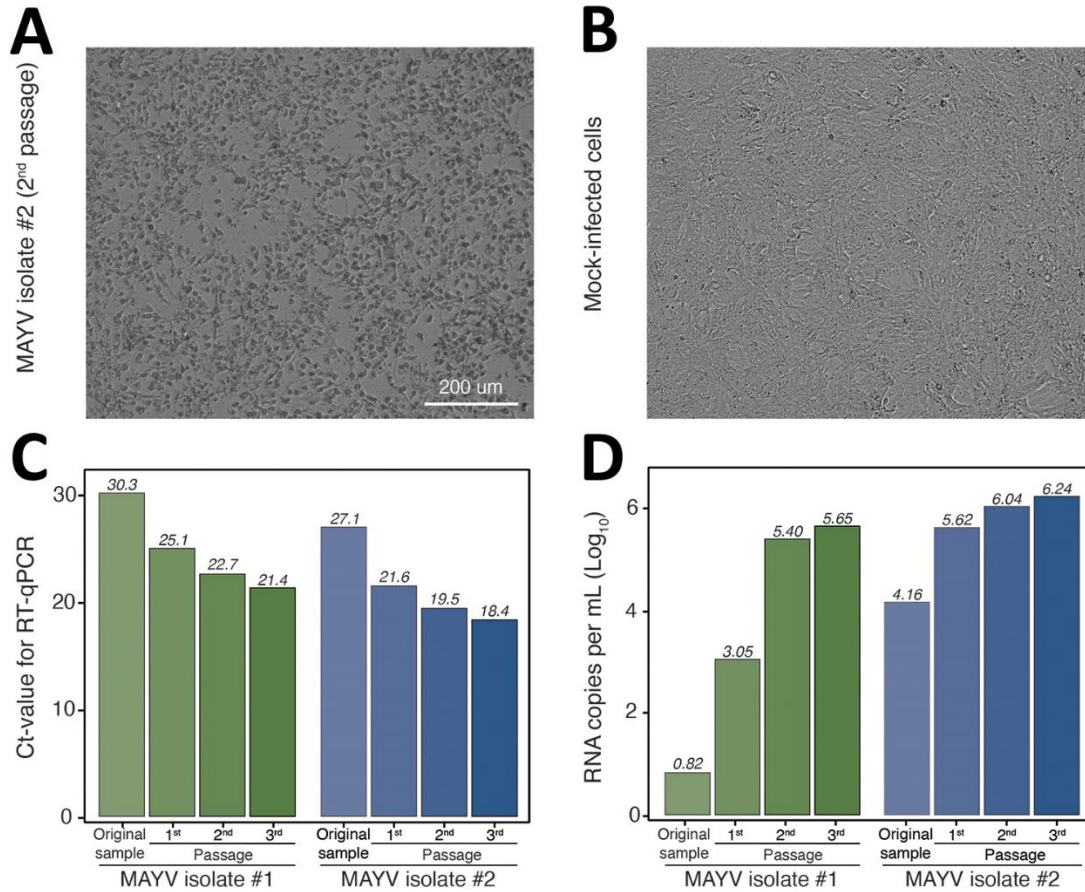
Appendix Figure 1. Molecular epidemiology of Mayaro virus in Roraima State, Brazil. Percentage of PCR-positive cases per fever cases tested for arboviruses (MAYV, CHIKV, DENV-1, and DENV-2) per month in Roraima State, Brazil between 2018 and 2021.



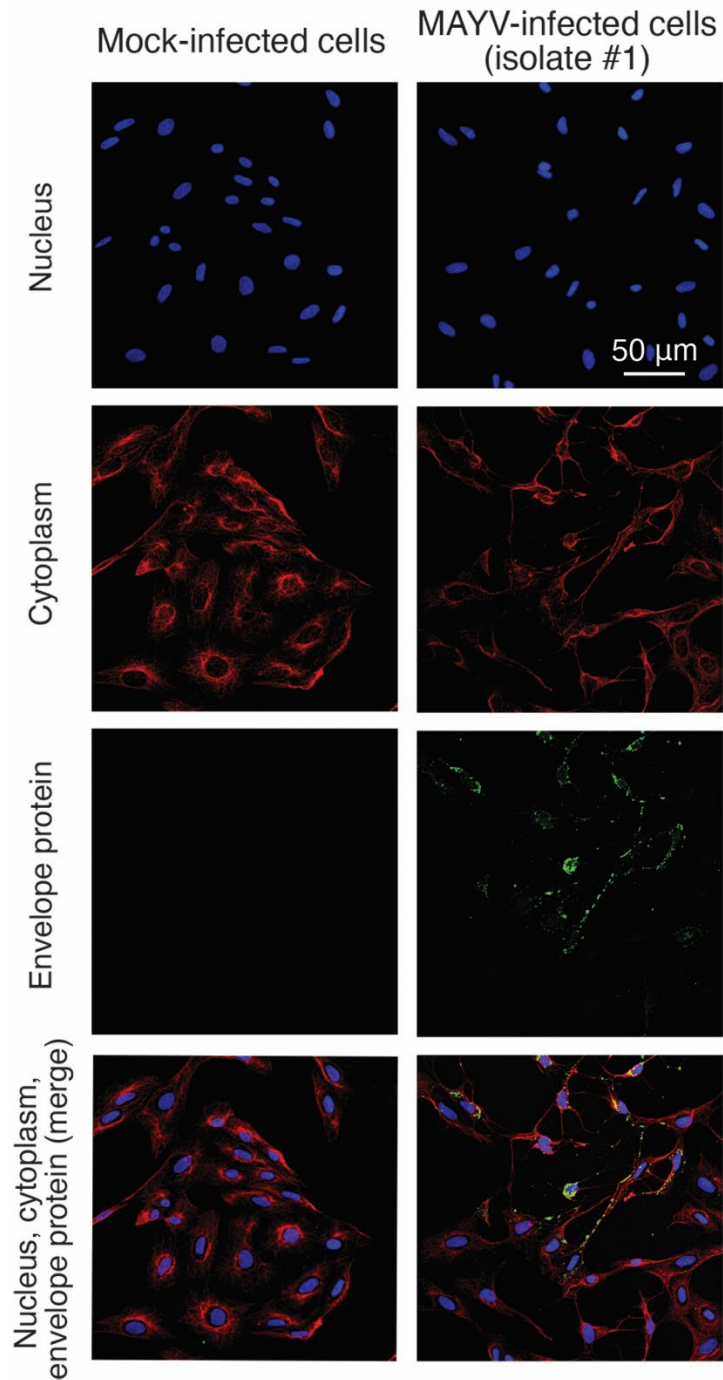
Cumulative MAYV cases (%):



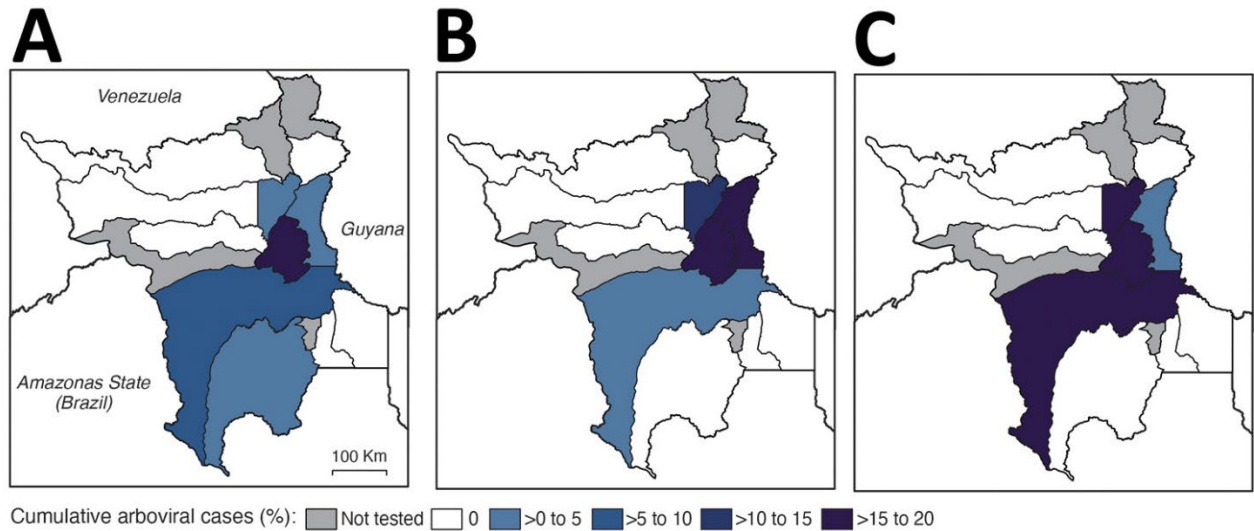
Appendix Figure 2. Molecular epidemiology of Mayaro virus in Roraima State, Brazil. Map of cumulative percentage of MAYV-positive cases per municipality in Roraima State between 2018 and 2021. The frequency of MAYV-positive samples per municipality was: Amajari (0%, 0/3), Alegre Alto (0%, 0/4), Boa Vista (3,9%, 15/384), Bonfim (0%, 0/40), Cantá (0%, 0/4), Caracará (9%, 2/23), Caroebe (13%, 1/8), Mucajaí (8%, 1/13), Normandia (0%, 0/5), Rorainópolis (3,5%, 6/172) and São João da Baliza (1,4%, 1/74). No samples from Iracema, Pacaraima, São Luiz, or Uiramutã were tested. Additionally, 92 patients had no information regarding their municipality of residence, including 2 positive samples.



Appendix Figure 3. Mayaro virus isolates in culture cells obtained from serum samples of febrile patients from Boa Vista municipality in 2020 and 2021, Roraima State, Brazil. MAYV isolates were obtained from patient RR-424 (isolate #1) and RR-58 (isolate #2) (A) Vero CCL-81 cells with the cytopathic effect caused by MAYV infection 30 hours post-infection. (B) Mock-infected Vero CCL-81 cells (negative control). (C). Cycle threshold (Ct)-value obtained by RT-qPCR from MAYV isolates and original samples. (D) Estimate MAYV RNA copies per mL obtained by RT-qPCR from MAYV isolates and original samples. MAYV, Mayaro virus.



Appendix Figure 4. Immunofluorescence of MAYV isolate. The images show staining of mock-infected Vero CCL81 cells and of Vero CCL81 cells inoculated with MAYV isolate #1 from patient RR-407. Cells were stained with antibodies against vimentin for visualization of the cytoplasm (red fluorescence, row 2), and MAYV envelope 2 protein (green fluorescence, row 3). Nuclei were labeled with Hoechst dye (blue fluorescence, row 1). Slides were analyzed by confocal microscopy, and images were merged with ImageJ (merge, row 4). MAYV, Mayaro virus. DENV, dengue virus. CHIKV, chikungunya virus.



Appendix Figure 5. Maps of distribution of chikungunya and dengue cases in Roraima State, Brazil. Cumulative percentage of positive cases of chikungunya (A), dengue serotype 1 (B), and dengue serotype 2 (C) per municipality in Roraima State between 2018 and 2021. The frequency of CHIKV-positive samples per municipality was: Amajari (0%, 0/3), Alegre Alto (0%, 0/4), Boa Vista (1%, 4/384), Bonfim (5%, 2/40), Cantá (0%, 0/4), Caracarái (9%, 2/23), Caroebe (0%, 0/8), Mucajaí, (0%, 0/13), Normandia (0%, 0/5), Rorainópolis (5%, 8/172) and São João da Baliza (0%, 0/74). The frequency of DENV1-positive samples per municipality was: Amajari (0%, 0/3), Alegre Alto (0%, 0/4), Boa Vista (13%, 50/384), Bonfim (5%, 2/40), Cantá (25%, 1/4), Caracarái (17%, 4/23), Caroebe (0%, 0/8), Mucajaí, (0%, 0/13), Normandia (0%, 0/5), Rorainópolis (0%, 0/172) and São João da Baliza (0%, 0/74). The frequency of DENV2-positive samples per municipality was: Amajari (0%, 0/3), Alegre Alto (0%, 0/4), Boa Vista (18%, 70/384), Bonfim (5%, 2/40), Cantá (25%, 1/4), Caracarái (9%, 2/23), Caroebe (0%, 0/8), Mucajaí, (0%, 0/13), Normandia (0%, 0/5), Rorainópolis (3,5%, 6/172) and São João da Baliza (1%, 1/74). No samples from Iracema, Pacaraima, São Luiz, or Uiramutã were tested. Additionally, 92 patients had no information regarding their municipality of residence, including 4 positive samples to DENV-1 and 12 to DENV-2. Km, kilometers.